Characterization of a C-terminal-type kinesin-related protein from *Dictyostelium discoideum*

Sosuke Iwai, Eigo Suyama, Hiroyuki Adachi, Kazuo Sutoh*

Department of Life Sciences, Graduate School of Arts and Sciences, University of Tokyo, 3-8-1 Komaba, Meguro-ku, Tokyo 153-8902, Japan

Abstract We have determined the full sequence of K2, a kinesin-related protein (KRP) in *Dictyostelium discoideum*. Sequence homology and domain organization placed K2 in the ncd/Kar3 subfamily of the C-terminal-type KRPs. Bacterially expressed, truncated K2 showed ATP-dependent binding to microtubules and microtubule-stimulated ATPase activity. K2-null cells grew and developed normally, suggesting overlapping functions of K2 with other microtubule motor(s). Overexpression of K2 caused partial mitotic arrest. Green fluorescent protein-tagged full-length K2 localized in the nucleus at the interphase and on the mitotic spindle during mitosis. These results suggest that K2 is a microtubule-dependent motor which may play some roles in mitotic spindles. © 2000 Federation of European Biochemical Societies. Published by Elsevier Science B.V. All rights reserved.

Key words: Kinesin-related protein; C-terminal-type kinesin; Mitotic spindle; *Dictyostelium discoideum*

1. Introduction

The kinesin superfamily is a group of motor proteins that convert energy generated by hydrolysis of ATP into movement along microtubules. Since the first isolation of kinesin [1], dozens of related proteins (kinesin-related proteins, KRPs) have been identified from a wide range of eukaryotic cells and shown to be involved in a variety of intracellular functions including vesicle and organelle transport, mitotic spindle morphogenesis, and chromosome separation. KRPs share a conserved motor domain that contains ATP and microtubule binding sites. Outside the motor domain, KRPs show significant sequence diversity, which is responsible for functional diversity. Although many KRPs have N-terminal motor domains and move toward the plus end of the microtubule, some KRPs, like *Drosophila* ncd and *Saccharomyces cerevisiae* Kar3, have C-terminal motor domains and move toward the minus end of the microtubule [2–4].

The cellular slime mold *Dictyostelium discoideum* is a simple eukaryote which serves as a model system for studying cytoskeletons and motor proteins. By using this unicellular organism, it is possible to characterize genes by genetic approaches such as gene disruption and overexpression. In addition, *Dictyostelium* cells show various cellular functions, including chemotactic cell movement and multicellular development. *Dictyostelium* KRPs are also expected to have functional and structural diversity corresponding to their cellular functions. Previously, short DNA fragments encoding six *Dictyostelium* KRPs were isolated using a PCR-based strategy. The full sequence of one of them, K7, was reported [5]. Moreover, by using in vitro organelle transport assays, two types of *Dictyostelium* KRPs were biochemically purified, and the full sequence of one of them, DdUnc104, was reported [6]. It has been shown that K7 plays a role in the developmental process of *Dictyostelium* cells upon starvation [5] and that DdUnc104 is required in organelle transport [6]. However, structures and functions of other *Dictyostelium* KRPs remain to be determined.

In this paper, to further investigate *Dictyostelium* KRPs, we determined the full sequence of K2, one of the *Dictyostelium* KRPs whose partial sequence has been previously reported [5]. From sequence homology and domain organization, K2 thus sequenced was grouped in the ncd/Kar3 subfamily of the C-terminal-type KRPs. K2 is the first C-terminal-type KRP ever discovered in *Dictyostelium* cells. For further characterization, we expressed K2 in *Escherichia coli* cells and examined its biochemical properties. We also examined phenotypic changes of *Dictyostelium* cells upon disruption or overexpression of the K2 gene. Furthermore, the intracellular localization of K2 was examined by using the green fluorescent protein (GFP)-tagged protein.

2. Materials and methods

2.1. Determination of the full sequence of the K2 gene

Starting from the sequence of a K2 fragment ($\sim$1 kb) previously reported [5], genomic walking was performed by inverse PCR on the genomic DNA isolated from *Dictyostelium* Ax2 cells. After three rounds of walking, DNA fragments spanning the whole K2 gene were obtained (Fig. 1). For each amplified fragment, the sequences of several clones were determined to obtain the full sequence of the K2 gene. Full-length cDNA clones were obtained by 3′-rapid amplification of cDNA ends (RACE) and reverse transcription (RT) PCR from the total RNA purified from vegetative Ax2 cells.

2.2. Disruption of the K2 gene

A cDNA fragment ($\sim$1.8 kb) was amplified from the K2 cDNA by PCR using the primers containing restriction enzyme sites for *Eco*RI. A blasticidin S resistance marker (Bsr) was taken from pUCBsrΔBam [7] and inserted into the unique *Nde*I site of the cDNA fragment to make the gene disruption construct (Fig. 1). The plasmid was digested with *Eco*RI and introduced into Ax2 cells by electroporation. Transformants were selected in the presence of 10 µg/ml blasticidin S. Independent clones were isolated, and disruption of the K2 gene in these clones was confirmed by Southern blot and RT-PCR.

2.3. Expression of K2 in Dictyostelium cells

The cDNA of the full-length K2 was fused either to the *Dictyostelium* actin 15 promoter or to the *Dictyostelium* discoidin promoter

*Corresponding author. Fax: (81)-3-5454 6751.
E-mail: sutoh@bio.c.u-tokyo.ac.jp

(*dis*1γ) and then inserted into a multicopy extrachromosomal vector, pBIG, to induce expression of K2 (Fig. 2). To produce GFP-K2 (Fig. 2), the GFP gene was inserted between the promoter and the K2 gene. The expression vectors were introduced into Ax2 cells by electroporation. Transformants were selected in the presence of 10 μg/ml G418.

2.4. Microscopic observation of cells

Cells were fixed in methanol containing 1% formaldehyde for 5 min at −10°C and washed three times with phosphate-buffered saline (PBS). For the observation of nuclei, the cells were stained with PBS containing 0.1 μg/ml of 4′,6-diamidino-2-phenylindole (DAPI) for 30 min at 37°C, washed with PBS, and observed by Axivort 35 with a Plan-Neofluar ×100 oil immersion objective (Zeiss) with epi-fluorescence optics. To determine the relative amount of DNA in each nucleus, DAPI fluorescence images were captured, and the fluorescence intensity of each nucleus was measured by Argus-20 (Hamamatsu). Phase contrast images were also captured to measure the relative area of each cell by Argus-20.

2.5. Expression of truncated K2 in E. coli cells

The cDNA encoding the K2 motor domain plus a part of the stalk of K2 (K2-390, amino acids 390–792) was amplified from the K2 cDNA by PCR. Double-stranded oligonucleotides for the Flag tag were inserted after the six-histidine tag sequence in the expression vector pET15b (Novagen). Subsequently, the PCR-amplified sequence was inserted into the resulting vector for expression of K2-390 (Fig. 2). *E. coli* cells (BL21(DE3)) transformed with this expression construct were grown at 37°C in 500 ml of LB until cell density reached $OD_{600} = 1$. The expression of K2-390 was then induced by addition of 0.4 mM isopropyl-1-thio-β-D-galactopyranoside. The cells were further grown for 4 h at 22°C and then harvested by centrifugation. They were resuspended in 10 ml of a lysis buffer (150 mM NaCl, 20 mM K_2PIPES (pH 7.0), 4 mM $MgSO_4$, 1 mM EGTA, 1 mM β-mercaptoethanol, 1 mM phenylmethylsulfonyl fluoride) containing 10 mM imidazole and sonicated on ice. After centrifugation for 30 min at $10\,000 \times g$, the supernatant was mixed gently with 1.5 ml of nickel-nitrilotriacetic acid resin (Qiagen) for 1 h at 4°C. The resin was precipitated by centrifugation and then washed twice with a lysis buffer containing 50 mM imidazole. The resin was precipitated again, and bound proteins were eluted with 2 ml of a lysis buffer containing 300 mM imidazole. The eluate was dialyzed against an 80PEM buffer (80 mM K_2PIPES (pH 7.0), 4 mM $MgSO_4$, 1 mM EGTA, 1 mM dithiothreitol) or a K-acetate buffer (10 mM Tris-acetate (pH 7.5), 50 mM K-acetate, 4 mM $MgSO_4$, 1 mM EGTA, 1 mM dithiothreitol) and finally centrifuged at $100\,000 \times g$ for 20 min to remove the aggregate. The purity of K2-390 was determined by SDS–PAGE. The concentration of the purified K2-390 was determined with protein assay reagent (Pierce).

2.6. Microtubule pelleting assay

Tubulin was purified as described previously [8]. For the microtubule pelleting assays, K2-390 (final concentration, 100 μg/ml) was mixed with taxol-stabilized microtubules (final concentration,

300 μg/ml) or buffer in 80PEM buffer supplemented with 10 mM AMPPNP and 10 mM $MgSO_4$. After 20 min incubation at room temperature, the mixtures were centrifuged for 30 min at $100\,000 \times g$ at 22°C to separate microtubule pellet and supernatant. For the ATP-dependent release experiment, the pellet was resuspended in release buffer (100 mM K_2PIPES (pH 7.0), 100 mM NaCl, 10 mM $MgSO_4$, 1 mM EGTA). The resuspended pellet fraction was divided in two, and one of them was supplemented with 10 mM ATP. After 20 min incubation at room temperature, the mixtures were recentrifuged.

All supernatant and pellet fractions were analyzed with SDS–PAGE. The K2-390 bands on the gel were visualized by immunoblotting with anti-Flag antibody because tubulin migrated very close to K2-390. SDS–PAGE and electrophoretic transfer were carried out according to standard method. The blots were blocked for 1 h in TBST (20 mM Tris (pH 8.0), 150 mM NaCl, 0.1% Tween 20) containing 1% blocking reagent (Boehringer Mannheim) and then incubated in TBST containing 10 μg/ml of anti-Flag M2 monoclonal antibody (Sigma), followed by alkaline phosphatase-conjugated secondary antibody (1:2000) (Vector Laboratories). Blots were rinsed and developed with CDP-star (Amersham Pharmacia).

2.7. ATPase assay

K2-390 (final concentration, 20 μg/ml) was mixed with various concentrations of taxol-stabilized microtubules in 108 μl of a K-acetate buffer. The ATPase reaction was initiated by addition of 12 μl of 10 mM ATP. After various periods at 25°C, 20 μl of the reaction mixture was drawn, and the reaction was stopped by addition of 80 μl of 0.3 M perchloric acid. Amounts of released phosphate were determined by the modified malachite green method [9] and plotted against the reaction time to determine the rate of phosphate release.

3. Results

3.1. The K2 gene and its gene product

The entire K2 gene as well as its cDNA was cloned and sequenced as described in Section 2. The K2 gene composed of 2475 bp had one open reading frame interrupted by one intron (Fig. 1). The location of the intron was confirmed from the sequence of cDNA. The gene was predicted to encode a protein of 792 amino acid residues, as shown in Fig. 3. Sequence comparison with other KRPs showed that the putative motor domain of K2 was at the C-terminal region and had the highest degree of homology to the C-terminal-type kinesins, sharing 54% identity with *Xenopus* XCTK2 [10], 53% with *Arabidopsis* KatB [11], and 52% with *Aspergillus* KlpA [12]. Although outside the motor domain K2 did not show significant homology to other C-terminal-type kinesins, its structural organization was similar to that of ncd [13,14] and Kar3 [15]. In all of them, the central stalk region is ex-
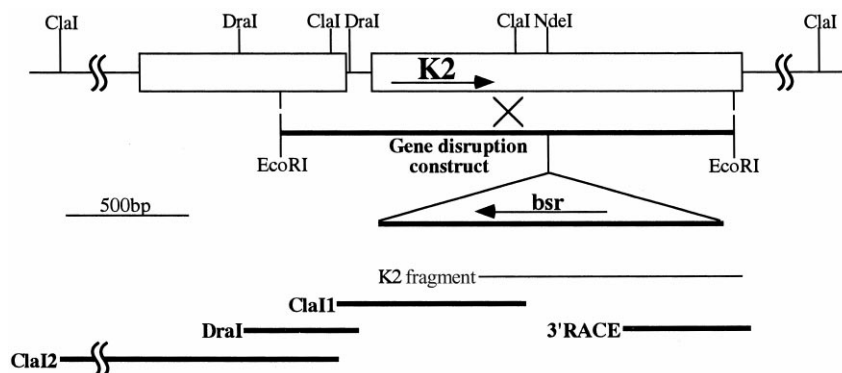

Fig. 1. Schematic representation of the K2 gene. Boxes represent exons of the K2 gene. A short intron (about 100 bp) interrupts the open reading frame of the K2 gene. K2 fragment: the previously sequenced [5] genomic DNA fragment. *Cla*I1, *Dra*I, and *Cla*I2: three inverse PCR products spanning the rest of the K2 gene. 3′RACE: the 3′RACE product. Gene disruption construct: the construct to disrupt the K2 gene by homologous recombination. In this construct, the Bsr gene is inserted at the *Nde*I site of the K2 gene.
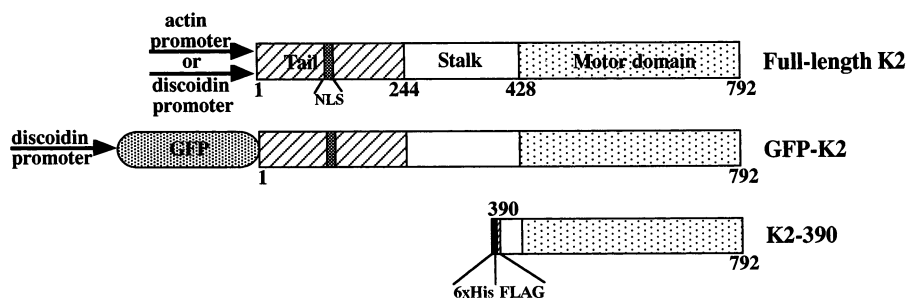
Fig. 2. Schematic representation of K2 or its fragments expressed either in *Dictyostelium* cells or in *E. coli* cells. Full-length K2 consists of three domains: the N-terminal tail containing the NLS, the central stalk, and the C-terminal motor domain. The full-length K2 was expressed in *Dictyostelium* cells either by the actin 15 promoter or by the discoidin promoter. K2 fused with GFP (GFP-K2) was also expressed in *Dictyostelium* cells by the discoidin promoter. The truncated K2 with the motor domain, a part of the stalk, and six-histidine/Flag tags (K2-390) was expressed in *E. coli* cells.

pected to form α-helical coiled coil, and the N-terminal tail region is rich in basic residues (calculated $pI \approx 10$). The tail region contained a putative nuclear localization signal (NLS) as indicated in Fig. 3.

3.2. Disruption of the K2 gene

To examine the cellular functions of K2, the K2 gene was disrupted by homologous recombination, as described in Section 2. The K2-null cells grew normally in suspension and showed normal morphology at the vegetative stage. In the course of development upon starvation, the null cells aggregated and formed fruiting bodies like wild-type Ax2 cells. These results imply the existence of other microtubule motor(s) with functions overlapping with those of K2.

3.3. Exogenous expression of K2 in wild-type Dictyostelium cells

To further examine the cellular functions of K2, the full-length K2 gene was fused to the *Dictyostelium* actin 15 promoter, one of the strongest *Dictyostelium* promoters, and expressed in wild-type Ax2 cells (Fig. 2). No transformant was obtained after antibiotic selection, suggesting that a high level of exogenous expression of K2 under control of the strong promoter was lethal. However, K2 was successfully expressed in wild-type cells under control of the discoidin promoter. This exogenous expression of K2 would have resulted in a moderate level of overexpression since the discoidin promoter is a weaker promoter than the actin 15 promoter. Among the cells expressing K2, about 10% showed abnormal morphol-

Fig. 3. Amino acid sequence of K2. K2 consists of 792 amino acid residues with a molecular mass of 89 kDa. The N-terminal tail, the central stalk, and the C-terminal motor domain are boxed. The putative NLS is underlined. The nucleotide sequence data reported in this paper will appear in the DDBJ/EMBL/GenBank nucleotide sequence databases with the accession number AB037280.
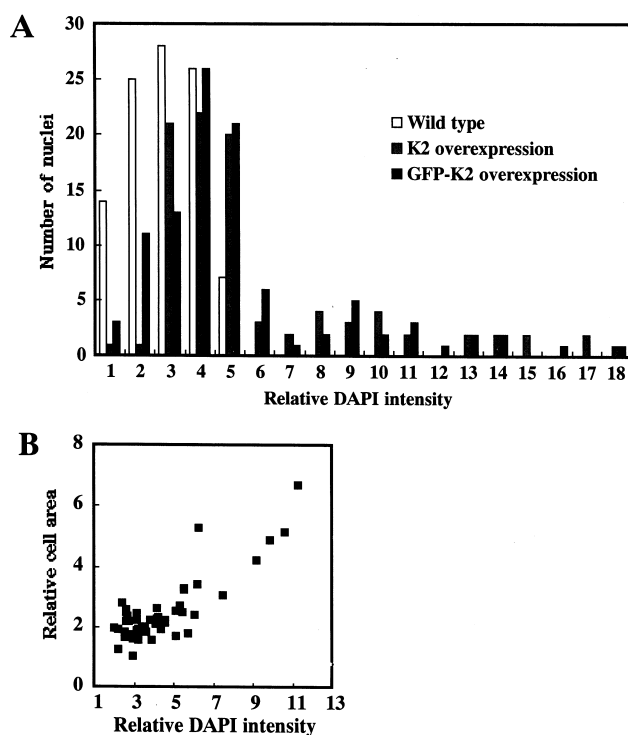
A

B

Fig. 4. Effect of a moderate level of expression of K2 in *Dictyostelium* cells. A: Distribution of relative amounts of DNA in each nucleus of wild-type cells and those expressing K2 or GFP-K2. B: Correlation between the amount of DNA and the size of cells expressing K2.

ogy, being several times as large as wild-type cells. DAPI staining showed that these large cells were all mononucleate, which indicates that this moderate level of overexpression of K2 by the discoidin promoter did not affect cytokinesis. However, simultaneous measurements of DNA content and cell size of those expressing K2 revealed that large cells contained several times as much DNA as wild-type cells (Fig. 4A,B), showing that a moderate level of overexpression of K2 caused partial mitotic arrest. A high level of overexpression of K2 was lethal, as shown above. These results show that the concentration of K2 in *Dictyostelium* cells must be strictly controlled.

3.4. Intracellular localization of GFP-tagged K2

To examine intracellular localization, full-length K2 was fused to GFP (GFP-K2) and expressed under control of the discoidin promoter (Fig. 2). This expression of GFP-K2 caused a partial mitotic arrest (Fig. 4A) that was similar to that observed by expression of K2 without GFP, indicating that GFP-K2 behaved like K2 in *Dictyostelium* cells. When fixed cells were examined, GFP-K2 showed nuclear localization in cells at the interphase (Fig. 5b) which coincides with DAPI staining (Fig. 5c). This localization is consistent with the presence of the putative NLS in the tail region of K2. In mitotic cells, however, GFP-K2 localized on mitotic spindles (Fig. 5d). GFP-K2 was enriched toward the spindle poles as compared to spindle microtubules.

3.5. Biochemical properties of bacterially expressed K2

To examine whether K2 shows the biochemical properties expected for a kinesin-related motor protein, the truncated
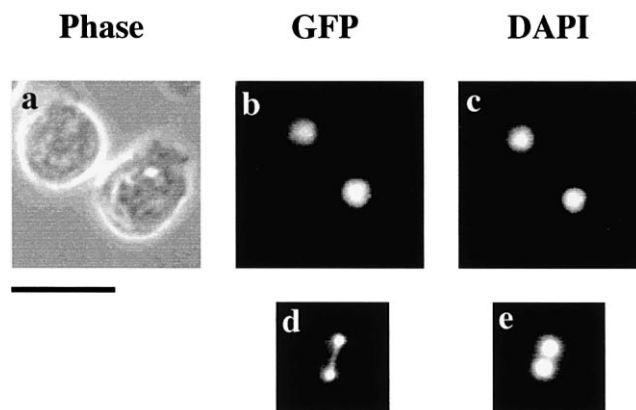

Fig. 5. Intracellular localization of GFP-K2. Cells at the interphase (a–c). A mitotic cell (d,e). Phase contrast image (a), GFP fluorescence images (b,d), and DAPI staining images (c,e). Bar, 10 μm.

K2, K2-390, consisting of the motor domain plus a part of the stalk of K2 ($\sim$45 kDa) with a fused six-histidine tag and a Flag tag at its N-terminus (Fig. 2), was expressed in *E. coli* cells. Determination of the molecular size of the purified K2-390 by gel chromatography indicated that most were dimers with a minor contamination of monomer.

Microtubule pelleting assays were performed to determine whether K2 binds to microtubules in vitro. The purified K2-390 was incubated with microtubules in the presence of 10 mM AMPPNP and centrifuged to precipitate microtubules with bound K2-390. Most K2-390 was precipitated with microtubules in the presence of AMPPNP (Fig. 6, +MTs+AMPPNP), whereas all of the K2-390 remained in the supernatant in the absence of microtubules (Fig. 6, −MTs). K2-390 was precipitated with microtubules in the presence of AMPPNP and the pellet was resuspended to release K2-390 from microtubules. Although almost all K2-390 remained on the microtubules in the absence of ATP (Fig. 6, −nucleotide), approximately one-third of the K2-390 was released from microtubules in the presence of 10 mM ATP (Fig. 6, +ATP). These experiments indicate that K2-390 binds to and is released from microtubules in a nucleotide-dependent manner at physiological ionic strength.
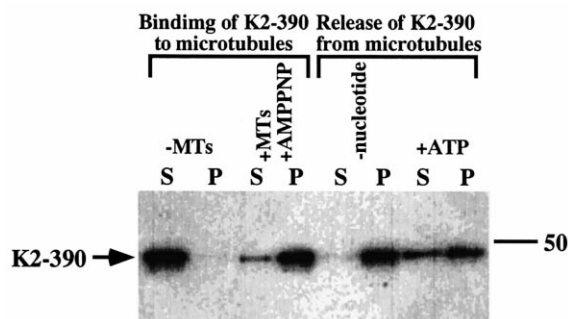

Fig. 6. Microtubule pelleting assays. K2-390 was incubated with microtubules (+MTs+AMPPNP) or buffer (−MTs) in the presence of AMPPNP and the mixtures were centrifuged. For the ATP-dependent release experiment, the microtubule–K2-390 complex was resuspended and divided in two. After incubation in the absence (−nucleotide) or presence (ATP) of ATP, the mixtures were recentrifuged. All supernatant (S) and pellet fractions (P) were analyzed with SDS–PAGE and immunoblotting.
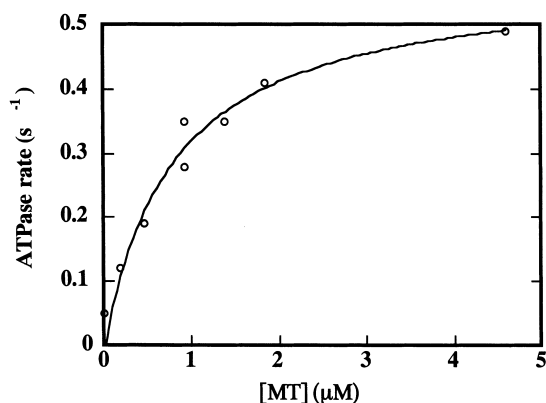
Fig. 7. Microtubule-stimulated ATPase activity of K2-390. The solid curve was calculated by assuming a Michaelis–Menten-type equation with a k_{cat} of 0.58 s^{-1} and a $K_{MT,0.5}$ of 0.81 μM.

Next, microtubule-stimulated ATPase activity of K2-390 was measured (Fig. 7). The maximum rate of ATP turnover per head (k_{cat}) of K2-390 was 0.58 s^{-1}, a value close to that of ncd [16]. The bimolecular rate constant, $k_{cat}/K_{MT,0.5}$, where $K_{MT,0.5}$ is equal to the concentration of tubulin dimers that produce a half-maximal ATPase rate, is often used as a kinetic index of processivity [16]. The $k_{cat}/K_{MT,0.5}$ value of K2-390 was about 1 μM^{-1} s^{-1}, suggesting that only a small number of ATP molecules is hydrolyzed per diffusional encounter with the microtubule, as in the case of ncd [16].

4. Discussion

From sequence homology of the motor domain, K2 was grouped in the ncd/Kar3 subfamily of the C-terminal-type KRPs. Although K2 does not show any sequence homology to ncd/Kar3 members outside the motor domain, K2 has structural features in common with them beyond this domain. First, the central stalk region is predicted to form an α-helical coiled coil, consistent with the observation that most of the bacterially expressed truncated K2 was dimers. Second, the N-terminal tail region is enriched in basic residues, which is thought to be involved in binding to the negatively charged region of the microtubule.

Bacterially expressed, truncated K2 showed ATP-dependent microtubule binding and microtubule-stimulated ATPase activity like other KRPs. Although in vitro microtubule gliding assays have shown that ncd and Kar3 are minus-end-directed motors [2–4], we failed to observe the gliding of microtubules on K2 proteins in vitro, possibly because the truncated K2 failed to adhere to the glass surface in an appropriate orientation to drive the gliding. However, considering our finding

that the truncated K2 hydrolyzes only a small number of ATP molecules per diffusional encounter with a microtubule, K2 could be a non-processive motor like other ncd/kar3 subfamily members.

The ncd/Kar3 subfamily members are thought to function in mitotic spindle morphogenesis [17]. K2-null cells grew and developed normally. However, a high level of overexpression of K2 in *Dictyostelium* cells was lethal. A moderate level of overexpression generated cells with an abnormal level of nuclear DNA content, implying partial mitotic arrest. GFP-tagged K2 localized to the nuclei of cells at the interphase and to mitotic spindles during mitosis. These results suggest that K2 may function in mitotic spindles like other ncd/Kar3 subfamily members, although the phenotype of K2-null cells implies the existence of other microtubule motor(s) with functions overlapping with those of K2.

References

[1] Vale, R.D., Reese, T.S. and Sheetz, M.P. (1985) Cell 42, 39–50.
[2] Walker, R.A., Salmon, E.D. and Endow, S.A. (1990) Nature 347, 780–782.
[3] McDonald, H.M., Stewart, R.J. and Goldstein, L.S.B. (1990) Cell 63, 991–1000.
[4] Endow, S.A., Kang, S.J., Satterwhite, L.L., Rose, M.D., Skeen, V.P. and Salmon, E.D. (1994) EMBO J. 13, 2708–2713.
[5] de Hostos, E.L., McCaffrey, G., Sucgang, R., Pierce, D.W. and Vale, R.D. (1998) Mol. Biol. Cell 9, 2093–2106.
[6] Pollock, N., de Hostos, E.L., Turck, C.W. and Vale, R.D. (1999) J. Cell Biol. 147, 493–505.
[7] Adachi, H., Hasebe, T., Yosinaga, K., Ohta, T. and Sutoh, K. (1994) Biochem. Biophys. Res. Commun. 205, 1808–1814.
[8] Valee, R.D. (1986) Methods Enzymol. 134, 89–104.
[9] Kodama, T., Fukui, K. and Kometani, K. (1986) J. Biochem. 99, 1465–1472.
[10] Walczak, C.E., Verma, S. and Mitchison, T.J. (1997) J. Cell Biol. 136 (4), 859–870.
[11] Mitsui, H., Yamaguchi-Shinozaki, K., Shinozaki, K., Nishiwaki, K. and Takahasi, H. (1993) Mol. Gen. Genet. 238, 362–368.
[12] O'Connell, M.J., Meluh, P.B., Rose, M.D. and Morris, N.R. (1993) J. Cell Biol. 120, 153–162.
[13] McDonald, H.M. and Goldstein, L.S.B. (1990) Cell 61, 991–1000.
[14] Endow, S.A., Henikoff, S. and Soler-Neidziela, L. (1990) Nature 345, 81–83.
[15] Meluh, P.B. and Rose, M.D. (1990) Cell 60, 1029–1041.
[16] Crevel, I.M.-T.C., Lockhart, A. and Cross, R.A. (1997) J. Mol. Biol. 273, 160–170.
[17] Endow, S.A. (1999) in: Guidebook to Cytoskeletal and Motor Proteins (Kreis, T. and Vale, R., Eds.), pp. 403–408, Oxford University Press, New York.